FIRST-ORDER DIFFERENCE ENERGY REGULARIZATION FOR ENHANCING RECONSTRUCTION PERFORMANCE IN COMPRESSIVE SENSING OF FOOT-GAIT SIGNALS

Jeevan K. Pant and Sridhar Krishnan

Department of Electrical and Computer Engineering
Ryerson University
Toronto, ON, M5B 2K3, Canada
Email: {jeevan1.pant,krishnan}@ryerson.ca

ABSTRACT

A new method for the regularization of the objective function for the reconstruction of the foot-gait signal from compressively sensed measurements is proposed. The method is based on using the ℓ_2 norm of the first-order difference to regularize the objective function. The state-of-the-art first-order difference sparsity promoting algorithms can introduce transient artefacts in the signal. The proposed regularization helps to reduce such artefacts. Involved optimization can be solved by using a sequential optimization procedure. The resulting algorithm is useful for enhancing the quality of reconstructed signal, especially in the situations when the CS system is applied with extremely high compression ratio. Simulation results indicate that the proposed method can offer upto 2.81dB improvement in signal-to-noise ratio, 0.02 units improvement in structural similarity measure, and a marginal increase in the computational effort.

***Index Terms*—** Compressive sensing, Foot-gait signals, Signal reconstruction.

1. INTRODUCTION

Compressive sensing (CS) is an efficient technique for the acquisition of sparse signals [1][2][3]. It involves computationally expensive signal reconstruction process, and the algorithms tailored for promoting temporal correlation structure can offer effective reconstruction of physiological signals [4][5]. The block-sparse Bayesian learning bound-optimization (BSBL-BO) algorithm [6] has been effective for the reconstruction of ECG signals. The ℓ_p^d-regularized least-squares (ℓ_p^d-RLS) algorithm offers better signal reconstruction performance especially for higher values of compression ratio (CR) [4]. However, the ℓ_p^d-RLS algorithm introduces transient artefacts in the reconstructed signal when applied for a CS system with extremely high CR.

The authors would like to thank Natural Sciences and Engineering Research Council of Canada (NSERC) for supporting this research.

We propose a first-order difference energy minimization technique, called as the ℓ_2^d-minimization technique, for the reduction of artefacts introduced by the ℓ_p^d-RLS algorithm for high values of CR. The resulting algorithm called as the ℓ_p^d/ℓ_2^d-regularized least-squares (ℓ_p^d/ℓ_2^d-RLS) algorithm can be solved by using a sequential optimization procedure. The gradient and Hessian of the objective function in the involved optimization problem can be readily computed, hence a gradient descent based optimization algorithm can be conveniently applied. Simulation results indicate that the ℓ_p^d/ℓ_2^d-RLS algorithm offers improvement in the quality of reconstructed signals, at the cost of a marginal increase in the amount of computation.

2. BACKGROUND

In CS, a vector $\boldsymbol{x}$ of length N representing a signal segment and its M number of measurements $\boldsymbol{y}$ are interrelated as

$$\boldsymbol{y} = \boldsymbol{\Phi}\boldsymbol{x} \tag{1}$$

where $\boldsymbol{\Phi}$ is a measurement matrix of size $M \times N$, typically with $M \ll N$. Reconstruction of a vector $\boldsymbol{x}$ representing temporally correlated physiological signals, such as ECG and foot-gait signals, from the measurements $\boldsymbol{y}$ can be carried out by solving the ℓ_p^d-regularized least-squares (ℓ_p^d-RLS) problem [4]

$$\underset{\boldsymbol{x}}{\text{miminize}} \quad f(\boldsymbol{x}) = \tfrac{1}{2}\,||\boldsymbol{\Phi}\boldsymbol{x} - \boldsymbol{y}||_2^2 + \lambda f_p^d(\boldsymbol{x}) \tag{2}$$

where $f_p^d(\boldsymbol{x})$ is the ℓ_p^d-pseudonorm given by

$$f_p^d(\boldsymbol{x}) = \sum_{n=1}^{N-1} \Big[(x_n - x_{n+1})^2 + \epsilon^2\Big]^{p/2}. \tag{3}$$

In (2), the regularization parameter λ can be used to balance a trade-off between the fidelity of the solution $\hat{\boldsymbol{x}}$ of the problem in (2) for satisfying (1) and sparsity on the first-order difference of $\hat{\boldsymbol{x}}$. In (3), p is selected so that $0 < p \leq 1$ and ϵ

is a small positive scalar used to render the function $f_p^d(\boldsymbol{x})$ smooth.

As described in [4], the problem in (2) can be solved by using a sequential optimization (Seq. Opt.) procedure described as follows: (i) Select large initial values $\{\epsilon_1, \lambda_1\}$ and small target values $\{\epsilon_T, \lambda_t\}$ of parameters $\{\epsilon, \lambda\}$. (ii) Compute a total of T monotonically decreasing sequences $\{\epsilon_1, \epsilon_2, \ldots, \epsilon_T\}$ and $\{\lambda_1, \lambda_2, \ldots, \lambda_T\}$ as

$$\epsilon_t = \epsilon_1 \exp\left[-\gamma(t-1)\right] \quad \text{for} \quad t = 1, 2, \ldots, T \tag{4a}$$

$$\lambda_t = \lambda_1 \exp\left[-\alpha(t-1)\right] \quad \text{for} \quad t = 1, 2, \ldots, T \tag{4b}$$

where $\gamma = \log(\epsilon_1/\epsilon_T)/(T-1)$ and $\alpha = \log(\lambda_1/\lambda_T)/(T-1)$. (iii) Implement the Seq. Opt. procedure by repeating the following steps for $t = 1, 2, \ldots, T$:

Step 1 For $t = 1$, set $\boldsymbol{x}_s = \mathbf{0}$; for $t > 1$, select the solution obtained from the $(t-1)$th sub-optimization as $\boldsymbol{x}_s$.

Step 2 Use $\boldsymbol{x}_s$ as the initializer, and carry out the tth sub-optimization by solving the problem in (2) with $\{\epsilon, p\} = \{\epsilon_t, p_t\}$.

The process of using decreasing values of ϵ and λ while carrying out the Seq. Opt. can be called as ϵ-continuation and λ-continuation, respectively.

3. RECONSTRUCTION OF FOOT GAIT SIGNALS AND ℓ_P^D/ℓ_2^D-REGULARIZED LEAST-SQUARES

Consider a foot-gait signal $\boldsymbol{x}$ shown in Fig. 1(a). The signal reconstructed from CS measurements $\boldsymbol{y}$ with CR$=95\%$ by applying the ℓ_p^d-RLS algorithm [4] is shown in Fig. 1(b). The first-order difference vectors of the original signal in Fig. 1(a) and that of the reconstructed signal in Fig. 1(b) are shown in Figs. 1(c) and 1(d), respectively. As can be seen, the reconstructed signal contains transient artefacts which can also be observed in Fig. 1(d) as components with large amplitudes relative to those shown in Fig. 1(c). Transient artefacts become conspicuous especially when CR is extremely high, and they affect the morphology of the signal. Therefore, we aim to reduce the transient artefact in the reconstructed signal by reducing the energy of the first-order difference vector, i.e., by reducing the ℓ_2 norm of the first-order difference vector. Below the ℓ_2 norm of the first-order difference vector will be called as the ℓ_2^d norm.

The ℓ_2^d-norm of $\boldsymbol{x}$, denoted as $f_2^d(\boldsymbol{x})$, is given by

$$f_2^d(\boldsymbol{x}) = \sum_{n=1}^{N-1} (x_n - x_{n+1})^2 .$$

Function $f_2^d(\boldsymbol{x})$ can be included in the objective function $f(\boldsymbol{x})$ used in (2) as an additional regularization function. As a result, we consider the combined ℓ_p^d and ℓ_2^d-regularized least-squares optimization problem, called as the ℓ_p^d/ℓ_2^d-RLS optimization problem, given by

$$\underset{\boldsymbol{x}}{\text{minimize}} \quad f(\boldsymbol{x}) \tag{5a}$$

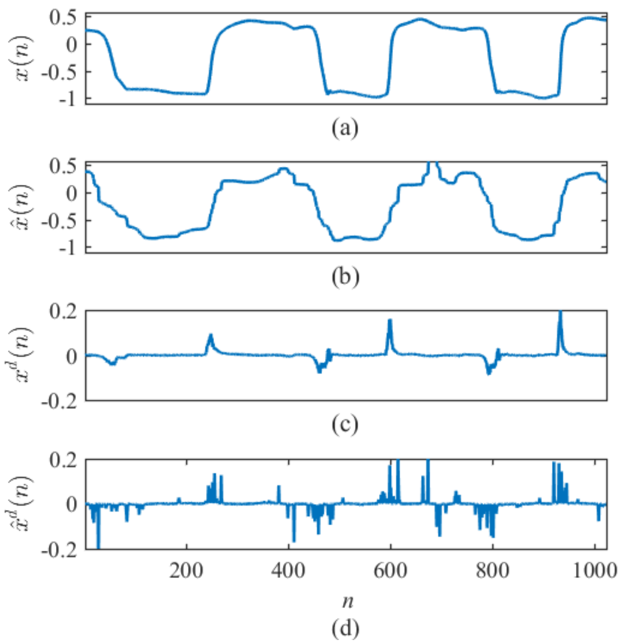

Fig. 1: (a) Original foot-gait signal, (b) signal reconstructed by using ℓ_p^d-RLS algorithm from measurements with CR$=95\%$, (c) first-order difference of the original signal, and (d) first-order difference of the reconstructed signal.

where

$$f(\boldsymbol{x}) = \frac{1}{2}\,||\boldsymbol{\Phi x} - \boldsymbol{y}||_2^2 + \lambda f_p^d(\boldsymbol{x}) + \mu f_2^d(\boldsymbol{x}), \tag{5b}$$

and λ and μ are the regularization parameters. Parameter λ can be used to promote sparsity on the first-order difference of $\boldsymbol{x}$ and μ can be used to reduce the transient artefacts resulting from the promotion of sparsity.

Gradient of $f(\boldsymbol{x})$ can be computed as

$$\boldsymbol{g} = \boldsymbol{\Phi}^T\left(\boldsymbol{\Phi x} - \boldsymbol{y}\right) + \lambda \boldsymbol{g}_p + \mu \boldsymbol{g}_2 \tag{6a}$$

where vector $\boldsymbol{g}_2$ is given by

$$\boldsymbol{g}_2 = \left[g_{2,1}\ g_{2,2}\ \cdots\ g_{2,N}\right]^T \tag{6b}$$

and

$$g_{2,n} = \begin{cases} 2\left(x_n - x_{n+1}\right) & \text{for } n = 1 \\ 2\left(-x_{n-1} + 2x_n - x_{n+1}\right) & \text{for } n = 2, \ldots, N-1 \\ 2\left(-x_{n-1} + x_n\right) & \text{for } n = N \end{cases} . \tag{6c}$$

Hessian matrix $\mathbf{H}$ of size $N \times N$ for $f(\boldsymbol{x})$ can be computed as

$$\mathbf{H} = \boldsymbol{\Phi}^T\boldsymbol{\Phi} + \lambda \mathbf{H}_p + \mu \mathbf{H}_2 \tag{7a}$$

where $\mathbf{H}_2$ is the Hessian for $f_2^d(\boldsymbol{x})$ whose $\{i, j\}$th component

$h_{i,j}$ is given by

$$h_{i,j} = \begin{cases} 1 & \text{for } \{i,j\} = \{1,1\}, \{N,N\} \\ 2 & \text{for } \{i,j\} = \{2,2\}, \ldots, \{N-1, N-1\} \\ -1 & \text{for } \{i,j\} = \{1,2\}, \ldots, \{N-1, N\} \\ -1 & \text{for } \{i,j\} = \{2,1\}, \ldots, \{N, N-1\} \\ 0 & \text{otherwise} \end{cases} . \tag{7b}$$

Gradient vector $\boldsymbol{g}_p$ and Hessian matrix $\mathbf{H}_p$ for the ℓ_p^d-pseudonorm $f_p^d(\boldsymbol{x})$ in (5b) are given in [4].

Using (6), (7), and the expressions for gradient and Hessian given in [4], a conjugate-gradient (CG) algorithm can be readily implemented for solving the problem in (5) for a given set of values of $\{\epsilon, \lambda, \mu\}$. For an implementation of the Seq. Opt. procedure (see last paragraphs of Sec. 2) for solving the problem in (5), we propose to include μ-continuation in addition to the $\{\epsilon, \lambda\}$-continuation. Thus, given sufficiently large and small values $\{\mu_1, \mu_T\}$ of μ, a total of T monotonically decreasing values of μ can be determined as

$$\mu_t = \mu_1 \exp\left[-\alpha(t-1)\right] \quad \text{for} \quad t = 1, 2, \ldots, T \tag{8}$$

where $\alpha = \log(\mu_1/\mu_T)/(T-1)$. In the resulting Seq. Opt. procedure, the tth sub-optimization can be carried out by solving the problem in (5b) with $\mu = \mu_t$, $\epsilon = \epsilon_t$, and $\lambda = \lambda_t$.

The ℓ_p^d/ℓ_2^d-regularized least-squares (ℓ_p^d/ℓ_2^d-RLS) algorithm based on the above analysis can be summarized as shown in Table 1.

Table 1: ℓ_p^d/ℓ_2^d-RLS Algorithm

Step 1:
Input $\boldsymbol{\Phi}$, $\boldsymbol{y}$, p, $\{\lambda_1, \lambda_T\}$, $\{\epsilon_1, \epsilon_T\}$, $\{\mu_1, \mu_T\}$, T.
Set $\boldsymbol{x}_s = \mathbf{0}$.
Step 2:
Compute $\{\epsilon_1, \ldots, \epsilon_T\}$, $\{\lambda_1, \ldots, \lambda_T\}$, $\{\mu_1, \ldots, \mu_T\}$ using (4), (8).
Step 3:
Repeat the following for $t = 1, 2, \ldots, T$:
(i) Set $\mu = \mu_t$, $\epsilon = \epsilon_t$, $\lambda = \lambda_t$.
(ii) Using initializer $\boldsymbol{x}_s$, gradient computed as (6), and Hessian computed using (7), run the tth sub-optimization with parameters μ, ϵ, λ .
(iii) Denote the resulting solution as $\boldsymbol{x}_s$.
Step 4:
Output $\boldsymbol{x}_s$ and Stop.

4. SIMULATION RESULTS

Segment length N was set to $N = 512$. The foot-gait signals were selected from the signal records in the Gait Dynamics in Neuro-Degenerative Disease database [7], and all the 128 signals were normalized so as to ensure that their their component values are within the range $-1 \leq x(n) \leq 1$. The signals were divided into segments of length N resulting in approximately 22000 segments. A total of 12 values of the number of measurements M were selected as $M = round(tN)$ where t = 0.05,0.08,. . .,0.38. A sparse random measurement matrix $\boldsymbol{\Phi}$ was constructed as in [4][5] with total two unity-valued components in each column. Measurements $\boldsymbol{y}$ were taken as (1). The proposed ℓ_p^d/ℓ_2^d-RLS and the ℓ_p^d-RLS [4] algorithms were applied with $T = 30$, $\epsilon_1 = 1$ $\epsilon_T = 10^{-3}$, $\lambda_1 = 1$, $\lambda_T = 10^{-3}$, $p = 1$. Parameters μ_1, μ_T for the ℓ_p^d/ℓ_2^d-RLS algorithm were set to $\mu_1 = 1$ and $\mu_T = 10^{-2}$. Signal-to-noise ratio (SNR) was computed as

$$\text{SNR} = 20\log_{10}\left(||\boldsymbol{x}||_2/||\boldsymbol{x} - \hat{\boldsymbol{x}}||_2\right) \text{ dB},$$

where $\hat{\boldsymbol{x}}$ denotes the reconstructed signal. Structural similarity index measure (SSIM) between vectors $\boldsymbol{x}$ and $\hat{\boldsymbol{x}}$ was computed as [8]

$$\text{SSIM}\left(\boldsymbol{x}, \hat{\boldsymbol{x}}\right) = l \cdot c \cdot s \tag{9a}$$

where

$$l = \frac{2m_{\boldsymbol{x}} m_{\hat{\boldsymbol{x}}} + 10^{-3}}{m_{\boldsymbol{x}}^2 + m_{\hat{\boldsymbol{x}}}^2 + 10^{-3}}, \quad c = \frac{2\sigma_{\boldsymbol{x}}\sigma_{\hat{\boldsymbol{x}}} + 10^{-3}}{\sigma_{\boldsymbol{x}}^2 + \sigma_{\hat{\boldsymbol{x}}}^2 + 10^{-3}}, \tag{9b}$$

$$s = \frac{\sigma_{\boldsymbol{x},\hat{\boldsymbol{x}}} + 10^{-3}}{\sigma_{\boldsymbol{x}}\sigma_{\hat{\boldsymbol{x}}} + 10^{-3}}. \tag{9c}$$

In (9), $m_{\boldsymbol{x}}$ and $m_{\hat{\boldsymbol{x}}}$ are mean values of $\boldsymbol{x}$ and $\hat{\boldsymbol{x}}$, respectively; and $\sigma_{\boldsymbol{x}}$, $\sigma_{\hat{\boldsymbol{x}}}$, and $\sigma_{\boldsymbol{x},\hat{\boldsymbol{x}}}$ denote standard deviation of $\boldsymbol{x}$, standard deviation of $\hat{\boldsymbol{x}}$, and covariance of $\boldsymbol{x}$, $\hat{\boldsymbol{x}}$, respectively. Compression ratio (CR) for a value of M was computed as

$$\text{CR} = \left[(N - M)/N\right] \times 100\%.$$

Average SNR obtained for the two algorithms over the reconstruction of 22000 different signal segments with different measurement matrices $\boldsymbol{\Phi}$ is shown in Fig. 2. As can be seen, SNR for the ℓ_p^d/ℓ_2^d-RLS algorithm is higher than that for the ℓ_p^d-RLS algorithm. Average SSIM is shown in Fig. 3. As can be seen, SSIM is higher for the ℓ_p^d/ℓ_2^d-RLS algorithm for all values of CR. SNR for ℓ_p^d/ℓ_2^d-RLS algorithm was observed to be more than that for the ℓ_p^d-RLS algorithm by upto 2.81dB. SSIM for the ℓ_p^d/ℓ_2^d-RLS algorithm for CR= 95% was observed to be higher than that for the ℓ_p^d-RLS algorithm, i.e., by 0.02 units higher than that for the ℓ_p^d-RLS algorithm.

Computational effort was measured in terms of the CPU time required to run a MATLAB R2016a implementation of an algorithm in a desktop PC with 2.20GHz processor, 8 GB RAM with 64−bit Windows 10 operating system. Average CPU time over 22000 different reconstructions is shown in Fig. 4. As can be seen, computational effort for the ℓ_p^d/ℓ_2^d-RLS algorithm is marginally higher than that for the ℓ_p^d-RLS algorithm. For CR=95%, CPU time for the ℓ_p^d/ℓ_2^d-RLS algorithm is smaller than that for the ℓ_p^d-RLS algorithm.

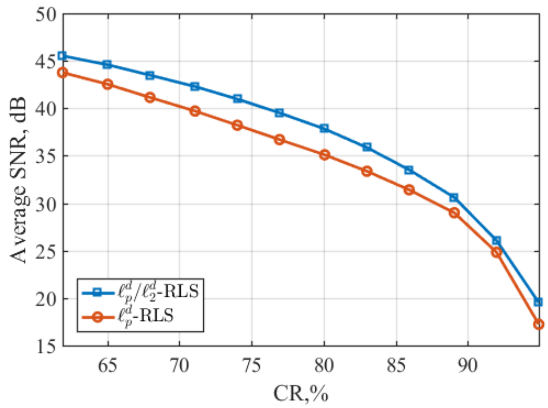

Fig. 2: SNR for foot-gait signals for ℓ_p^d/ℓ_2^d-RLS and ℓ_p^d-RLS algorithms with $N = 512$, over 22000 runs.

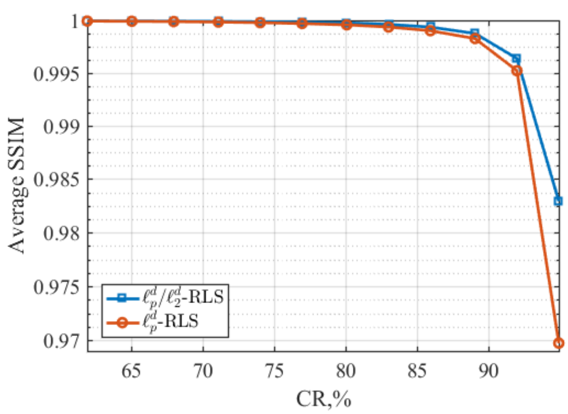

Fig. 3: SSIM for foot-gait signals for ℓ_p^d/ℓ_2^d-RLS and ℓ_p^d-RLS algorithms with $N = 512$, over 22000 runs.

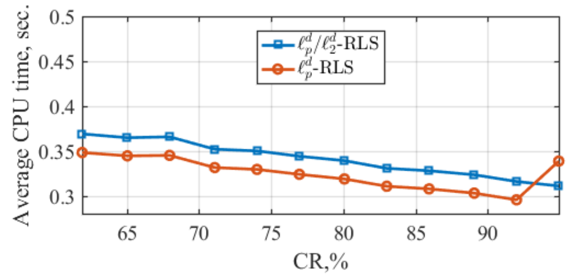

Fig. 4: Average CPU time for ℓ_p^d/ℓ_2^d-RLS and ℓ_p^d-RLS algorithms with $N = 512$, over 22000 runs.

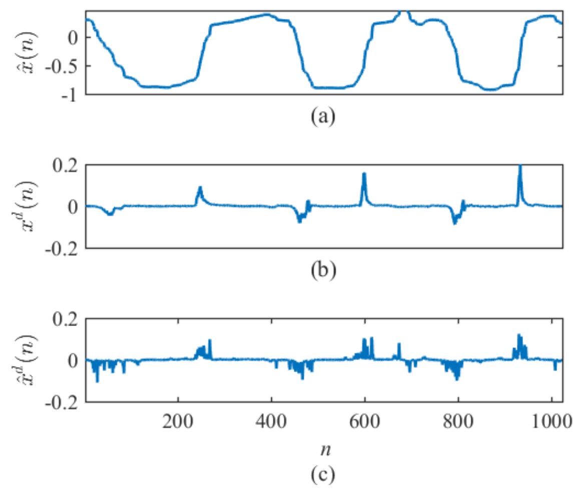

Fig. 5: (a) Signal reconstructed by using ℓ_p^d/ℓ_2^d-RLS algorithm from measurements with CR$=$ 95%, (b) first-order difference of the original signal in Fig. 1(a), and (c) first-order difference of the signal in (a).

Signal segment of length $N = 1024$ reconstructed by using the ℓ_p^d/ℓ_2^d-RLS algorithm with CR$=$ 95% is shown in Fig. 5; see Figs. 1(a) and 1(b) for corresponding original signal and signal reconstructed by using the ℓ_p-RLS algorithm, respectively. As can be seen, the quality of the signal reconstructed using ℓ_p^d/ℓ_2^d-RLS algorithm is much better than that reconstructed by using the ℓ_p^d-RLS algorithm. The FoD vector shown in Fig. 5(c) is closer to the FoD of original signal shown in Fig. 5(b) and Fig. 1(c) relative to the FoD vector shown in Fig. 1(b). SNR for the ℓ_p^d/ℓ_2^d-RLS and ℓ_p^d-RLS algorithms for the signals plotted in Figs. 1 and 5 were 14.65 and 11.26, respectively, and SSIM index for ℓ_p^d/ℓ_2^d-RLS and ℓ_p^d-RLS algorithms were 0.9779 and 0.94841, respectively.

4.1. Future work

In the proposed $f_{\ell_p^d}/f_{\ell_2^d}$-RLS algorithm, the energy minimization has been demonstrated to improve the performance of the ℓ_p^d-RLS algorithm [4] for extremely high values of CR. It would be interesting to study the effect of the energy minimization techniques for improving performance of the other related algorithms, such as, the ℓ_p^{2d}-RLS, $\ell_{2/p}^d$-RLS algorithms presented in [5][9][10].

5. CONCLUSION

A new method for the regularization of the objective function for the reconstruction of foot-gait signals is proposed. The ℓ_2^d-norm is used along with the ℓ_p^d-pseudonorm in the objective function of the involved optimization problem. Simulation results have indicated that the resulting ℓ_p^d/ℓ_2^d-RLS algorithm is effective for the reduction of transient artefacts introduced by the state-of-the-art ℓ_p^d-RLS algorithm. When CS is applied with extremely high compression ratio, the ℓ_p^d/ℓ_2^d-RLS algorithm can offer significantly higher SNR and SSIM index relative to the ℓ_p^d-RLS algorithm at the cost of a marginal increase in the computational effort.

6. REFERENCES

[1] E. Candès, J. Romberg, and T. Tao, "Robust uncertainty principles: exact signal reconstruction from highly incomplete frequency information," *IEEE Trans. Inf. Theory*, vol. 52, no. 2, pp. 489–509, Feb. 2006.

[2] E. Candès and T. Tao, "Near-optimal signal recovery from random projections: universal encoding strategies," *IEEE Trans. Inf. Theory*, vol. 52, no. 12, pp. 5406–5425, Dec. 2006.

[3] D. L. Donoho, "Compressed sensing," *IEEE Trans. Inf. Theory*, vol. 52, no. 2, pp. 1289–1306, Apr. 2006.

[4] Jeevan K. Pant and Sridhar Krishnan, "Reconstruction of ECG signals for compressive sensing by promoting sparsity on the gradient," in *Proc. IEEE Intl. Conf. Acoustics, Speech, and Signal Process.*, May 2013, pp. 993–997.

[5] Jeevan K. Pant and Sridhar Krishnan, "Compressive sensing of electrocardiogram signals by promoting sparsity on the second-order difference and by using dictionary learning," *IEEE Trans. Biomed. Circuits Syst.*, vol. 61, no. 3, pp. 198–202, Mar. 2014.

[6] Zhilin Zhang, Tzyy-Ping Jung, Scott Makeig, and Bhaskar D. Rao, "Compressed sensing of EEG for wireless telemonitoring with low energy consumption and inexpesive hardware," *IEEE Trans. Biomed. Engg*, vol. 60, no. 1, pp. 221–224, Jan. 2013.

[7] "Physionet: Gait dynamics in neurodegenerative disease database," . Available: https://physionet.org/physiobank/database/gaitndd/. [Accessed: 2017-09-15]

[8] Zhou Wang, Alan Conrad Bovik, Hamid Rahim Sheikh, and Eero P. Simoncelli, "Image quality assessment: From error visibility to structural similarity," *IEEE Trans. Image Process.*, vol. 13, no. 4, pp. 600–612, Apr. 2004.

[9] Jeevan K. Pant and Sridhar Krishnan, "Compressive sensing of foot gait signals and its application for the estimation of clinically relevant time series," *IEEE Trans. Biomed. Eng.*, vol. 63, no. 7, pp. 1401–1415, Jul. 2016.

[10] Jeevan K. Pant and Sridhar Krishnan, "Compressive sensing of ECG signals based on mixed pseudonorm of the first- and second-order differences," in *Proc. IEEE Intl. Conf. Acoustics Speech Signal Process*, May 2014, pp. 4423–4427.